Supplementary material for Hand muscles attachments: A Geometrical model

L. Havelková, T. Zítka, Fiala P., Rybarova M., R. Tupý, Kalis V., Ismail K. M.

21.7.2020

This material supplements article Hand muscles attachments: A Geometrical model and serves as dataset documentation as well. It summarizes data collected and describes in detail methods used. The dataset consists of two separate datasets: morphological and morphometric and dataset of positions of muscle lines origins, insertions and CSAs points. Methods described include Matlab code used to calculate lines end- and via-points and details on extractions of origin, insertion and CSA surfaces.

Contents

1 Morphological and morphometric dataset based on dissections

The morphological and morphometric dataset consist of morphological drawings (Figure 1 to 4) and tables 1 to 4 of morphometric dimensions available in `xlsx` files.

In Figure 1 trajectories and attachments of short flexors of thenar and hypothenar groups are shown, the abductor pollicis brevis is in the most lateral position of the thenar group and covers the opponens pollicis muscle. The adductor pollicis is the deepest and the most medial muscle of this group. The two heads (superficial and deep) of the flexor pollicis brevis are located at the centre of the group, separated by the tendon of flexor pollicis longus descending from the forearm.

In Figure 2 the origins, insertions and CSAs of the opponens pollicis and opponens digiti minimi are depicted. In the hypothenar group, the abductor digiti minimi is the most superficial and medial muscle. Flexor digiti minimi brevis is located at the centre of the group and covers the narrower belly of the opponens digiti minimi.

Figure 3 displays the long forearm muscles producing flexion at the wrist joint: the flexor carpi radialis and flexor carpi ulnaris. Flexor carpi ulnaris is the only muscle attached to the proximal row of carpal bones.

Figure 5 shows dimension of carpals bones complex measured based on MRI scan.

Table 1 summarizes the intrinsic muscles of the hand – four muscles of the thenar and six of the hypothenar group. Table 2 shows the central group of hand muscles – four dorsal interossei, three palmar interossei and four lumbricales. The origin areas of the dorsal interossei muscles are not clearly distinguishable, their fibres are located in narrow spaces between the metacarpal bones. Table 3 presents a selection of flexors and extensors from the extrinsic group of hand muscles.

Table 4 summarizes lengths of finger bones.

Table 1: dimensions of intrinsic hand muscle thenar and hypothenar group

See `table1.xlsx`

Table 2: dimensions of intrinsic hand muscle central group

See `table2.xlsx`

Table 3: dimensions of extrinsic hand muscles selected flexors and extensors

See `table3.xlsx`

Table 4: Lengths of finger bones

See `table8.xlsx`

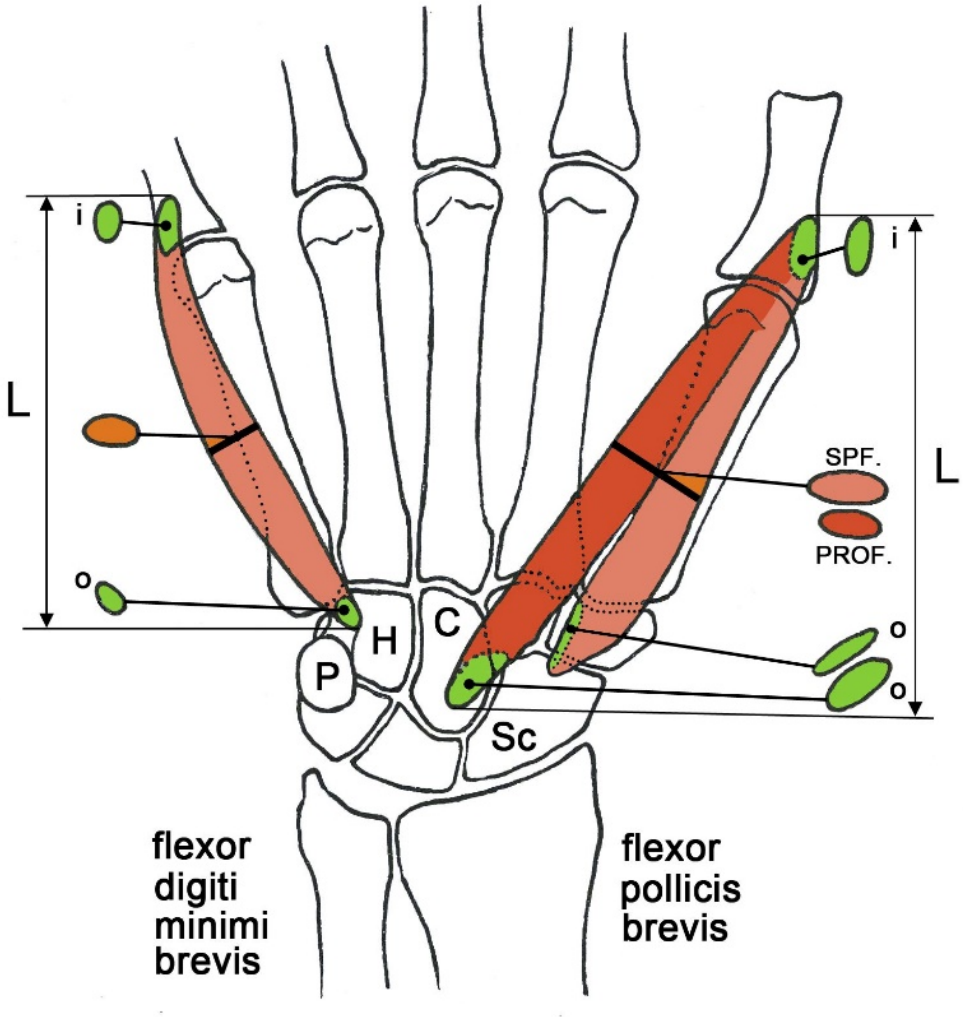

Figure 1: Origins and insertions of two short flexors of the thenar and hypothenar muscle group. Notes: L – muscle length, P – pisiform bone, H – hamate bone, C – capitate bone, Sc – scaphoid bone, o – muscle origin, i – muscle insertion, SPF – superficial muscle head, PROF – deep muscle head.

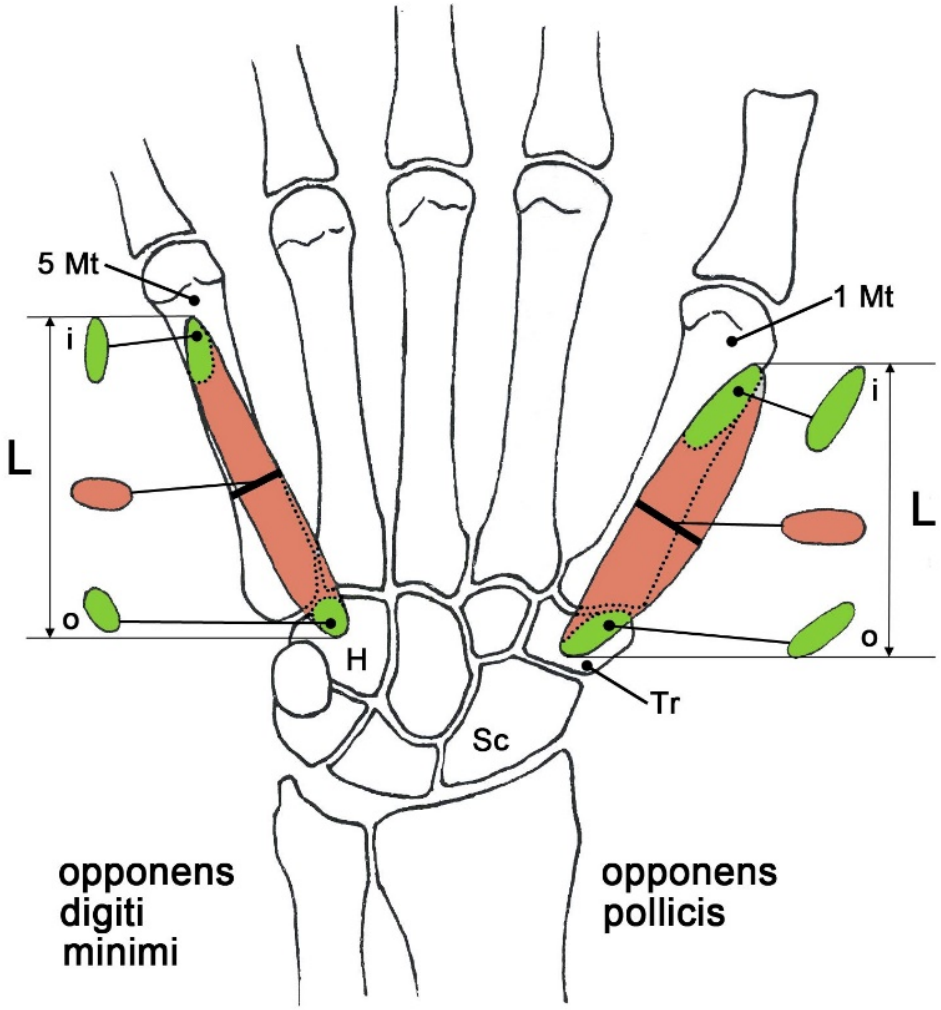

Figure 2: Origins and insertions of two muscles opposing the thumb (opponens pollicis) and the little finger (opponens digiti minimi). Notes: H – hamate bone, Sc – scaphoid bone, Tr – triquetrum bone, 1 Mt – first metacarpal bone, o – muscle origin, i – muscle insertion, L – muscle length.

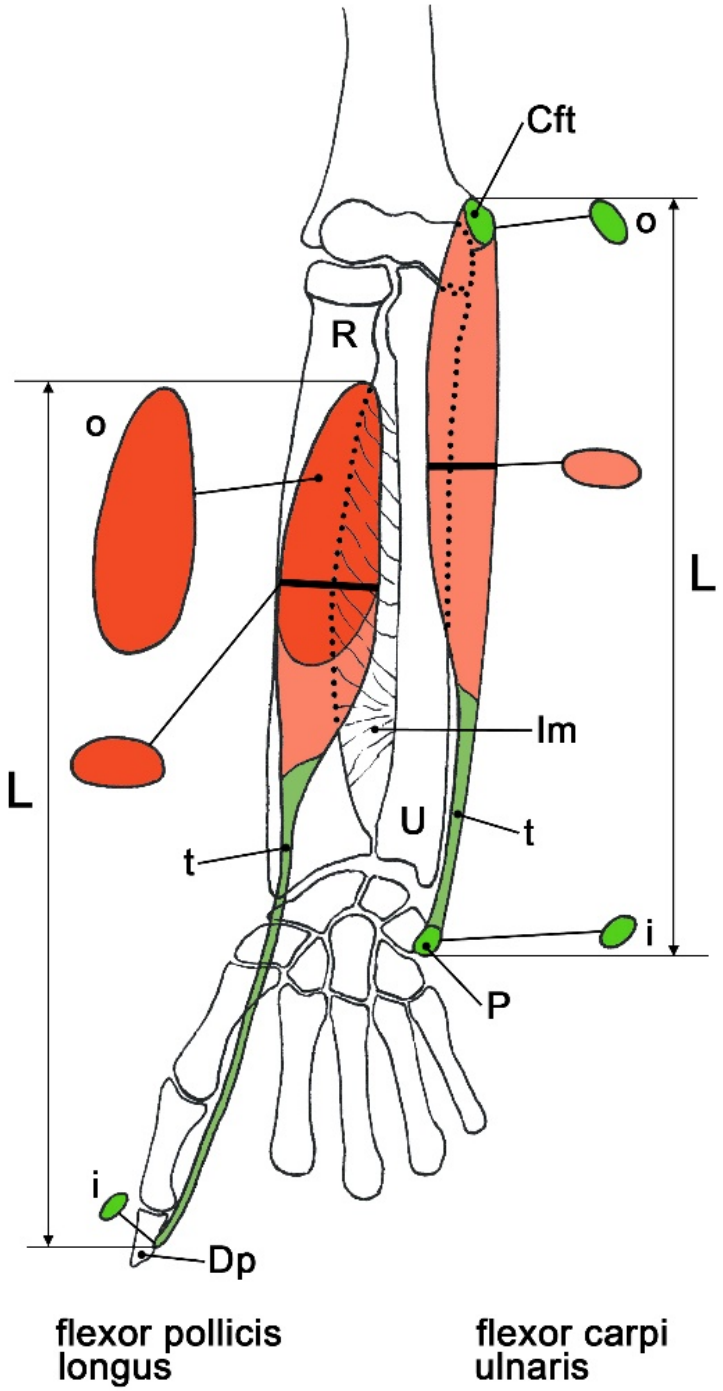

Figure 3: Origins and insertions of two extrinsic hand muscles – flexor pollicis longus and flexor carpi ulnaris. Notes: L – muscle length, t – tendon, o – origin, i – insertion, P – pisiform bone, CFT – common flexor tendon, Im – interosseous membrane, R – radius, U – ulna, Dp – distal phalanx.

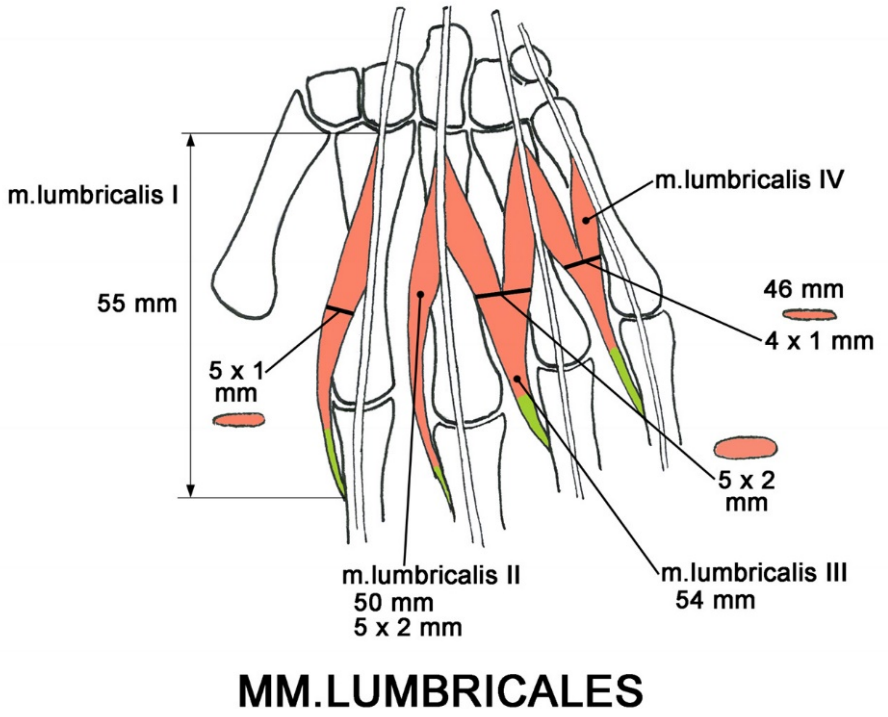

Figure 4: Measurements of length and biological cross section area for four lumbricales, tendons in green

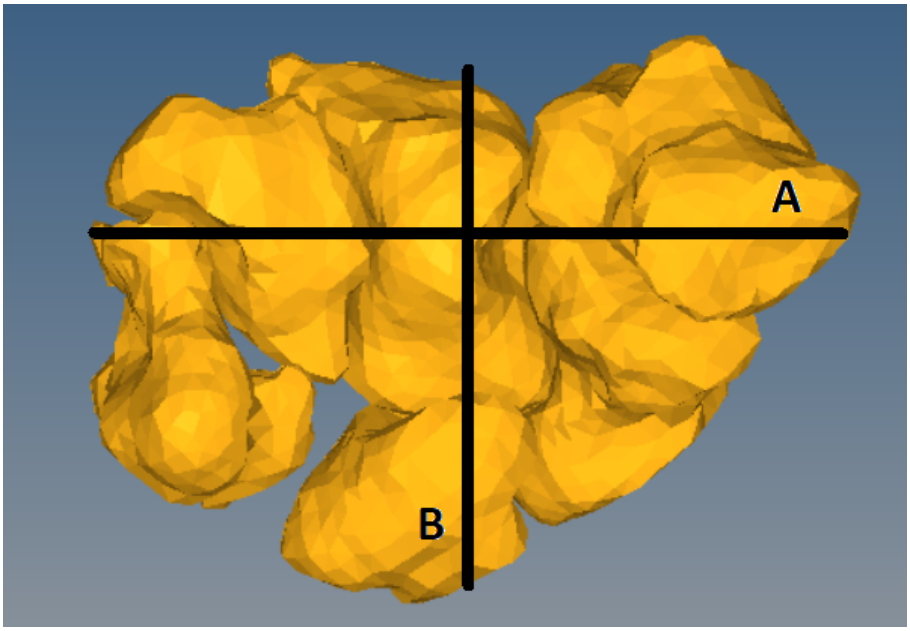

Figure 5: Dimensions of carpal bones complex, $A = 37.10\,mm$, $B = 55.83\,mm$

2 Placing muscle action lines

After obtaining the muscle origin surface, optional CSA surfaces and insertion surface, placing muscle action lines was undertaken in two stages:

(1) placing the required number of end points on origin and insertion surfaces and the same number of via-points on CSA surfaces [2, 5, 7] followed by

(2) pairing these points in order to specify individual action lines.

For the first task, modified k-means algorithm was used. Given a finite set of points $\omega \subset \mathbb{R}^N$ and natural number k original k-means method [4] iteratively tries to approximate solution to k-partition problem. That is to partition set ω into k classes $\omega_1, \dots \omega_k$ each corresponding with point $c_i \in \mathbb{R}^N$, $i = 1 \dots k$ called centroid, in such way that the expression

$$\sum_{i=0}^{k} \sum_{x \in \omega_i} \|c_i - x\|^2, \tag{1}$$

is minimal. In this setting, a set of centres of gravity of the triangles in the mesh is interpreted as the set ω. As the method is iterative it requires choosing initial set of centroids, in this case, the initial points are placed in centroids of largest triangles. The basic k-means method was modified in two ways. First, by ensuring that each centroid is always a point from ω by placing it in the closest point in ω after each iteration. Second, assigning a weight $w(x)$ equal to the surface volume of the corresponding triangle to each point $x \in \omega$ The generalized algorithm iteratively minimizes expression [1]

$$\sum_{i=0}^{k} \sum_{x \in \omega_i} w(x)\|c_i - x\|^2 \tag{2}$$

This ensures that the partition does not depend on density of points of the mesh, which might be affected by data acquisition process. Moreover, it ensures that the surface of the muscle attachment or CSA is divided between muscle elements so that the variation of surface volumes assigned to elements is minimal. Figure 6 (A) illustrates this partitioning, with triangles coloured according to the centroid their COG is assigned to.

Muscle elements' end or via-points were calculated separately for each surface. In order to place the muscle elements, corresponding points were connected so that lines of action neither intersect nor are entangled. Our approach was based on Euclidean matching problem in two dimensions. It can be proven that the minimality of total pairing distance ensures that no two line segments connecting paired points intersect and vice versa. This can be extrapolated to three dimensions. Nonetheless, It does not guarantee that action lines do not run over each other without intersecting. Fortunately, minimal matching still

provides good results in which virtual muscle elements are not tangled with each other. The minimal pairing was obtained by Hungarian algorithm [3], which computes minimal matching in weighted bipartite graph. In our study, we were concerned with complete bipartite graph on two sets of centroids on consecutive surfaces. Euclidean distances were taken as weights of the edges. This is complete bipartite graph, hence it contains perfect matching and minimal matching always exists [3].

Every such point was calculated in LCS of the corresponding bone, naturally respecting the real anatomy. The origin location and also the orientation of axes of the considered LCS are summarized in Table 5 and depicted in Figures 8, 9 and 10, based on previously published parameters [6].

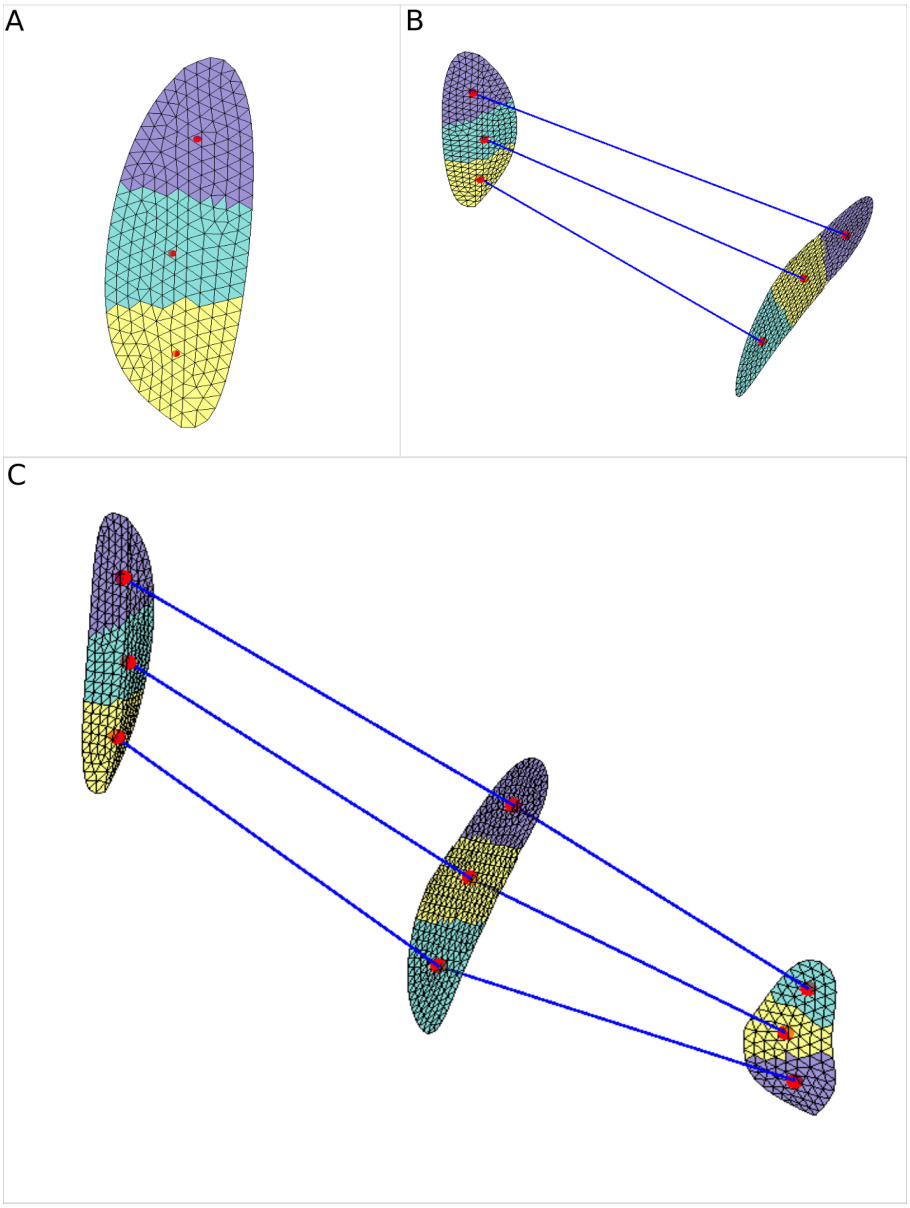

Figure 6: Adductor pollicis caput obliquum origin with five muscle elements endpoints and surfaces assigned to them coloured (A), connectivity of muscle origin and CSA surface with three muscle elements (B), connectivity of origin, CSA and insertion surface (C).

3 Dataset of positions of muscle lines origins, insertions and CSAs

The exact positions of muscle lines origins, insertions and CSAs dataset divided into archive files `muscle_paths_hand.zip`, `muscle_paths_shoulder.zip`, `muscle_paths_shoulder_deltoideus.zip`, `ligament_paths.zip` contains:

- all the attachment and intermediate surfaces extracted from MRI in binary `stl` format,
- calculated lines' end and via points in plain text csv files denoted by extension "`.asc`"

Data for individual muscles are organized into corresponding folders. Each folder contains:

- origin and insertion surfaces in `stl` files denoted by "`O`" and "`I`" in name respectively
- optionally intermediate CSA surfaces denoted by "`T`" or "`V`" resp. "`C`" in name, to specify connectivity surfaces are in order `O-I`, `O-T-I` or `O-V-C-I`

Points' order specifies their connectivity calculated based on Euclidean matching problem i.e. first points in `abductor_digiti_minimi_O_6_cntrds.asc` is paired with first point in `abductor_digiti_minimi_T_6_cntrds.asc` etc. Coordinates are in centimeters, data for individual axes are sorted naturally X, Y, Z. Coordinate system origin is illustrated in Figure 7.

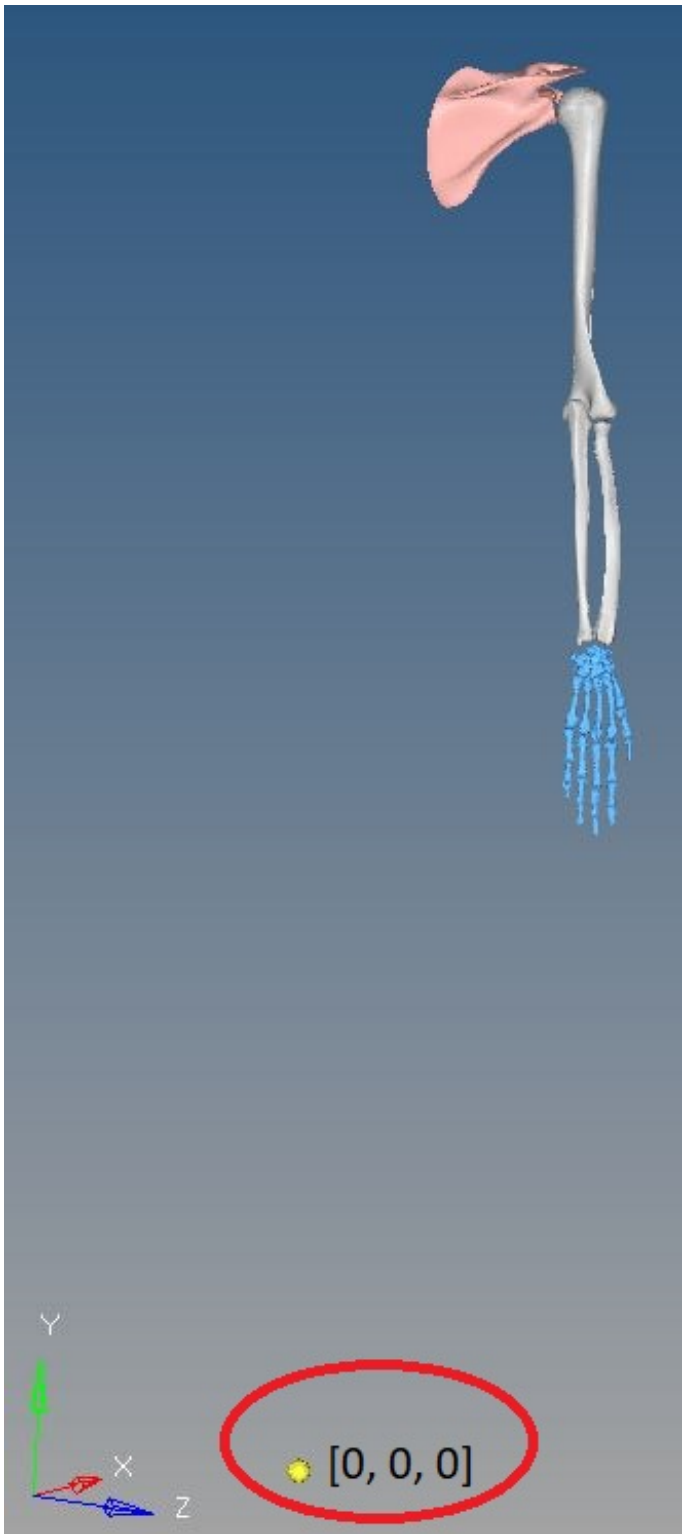

Figure 7: Coordinate system of MRI scans

Additionally, positions of points for some muscles transformed to local coordinate systems of appropriate bones are summarized in tables 5 to 6. Coordinate systems for individual segments can be found in Table 5 and Figures 8, 9 and 10.

Table 5: The LCS of individual segments – position of origin, axes orientation. Notes: COG – center of gravity; CSA – cross section area.

LCS	Position of origin	Axes orientation		
		X	Y	Z
Carpals	COG of segment	palmar	proximal	lateral
Finger phalanx	COG of segment	palmar	proximal	lateral
Humerus	centre of humeral head	lateral	proximal	posterior
Ulna	trochlear notch, on the right edge	medial	distal	posterior
Radius	in the centre of CSA of bone, in the level of radial tuberosity	proximal	medial	posterior

Table 6: origins/insertions intrinsic hand muscles thenar and hypothenar group

See `table5.xlsx`

Table 7: origins/insertions intrinsic hand muscles central group

See `table6.xlsx`

Table 8: origins/insertions extrinsic hand muscles selected flexors and extensors

See `table7.xlsx`

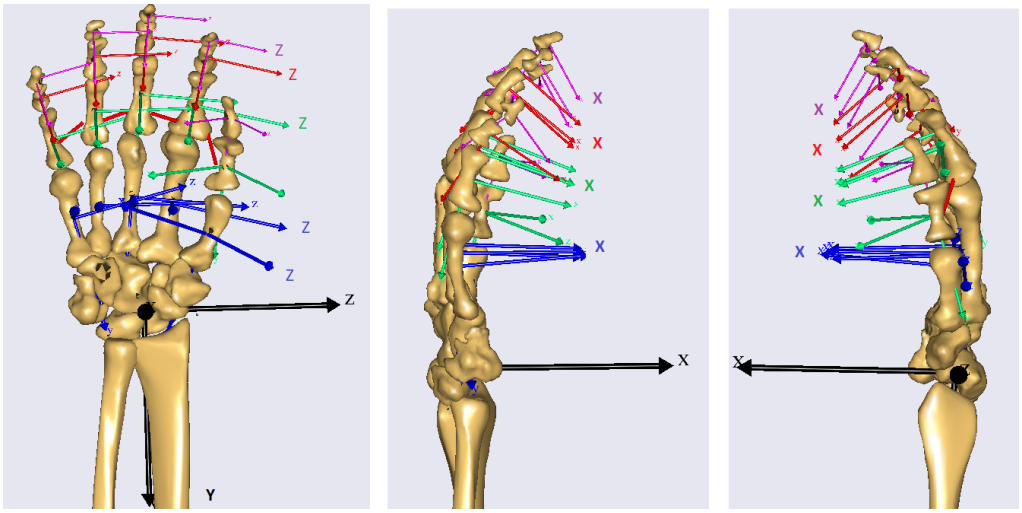

Figure 8: The local coordinate system of carpals and individual bones of the right hand. From the left: palmar view, pinky side view (medial), thumb side view (lateral). Notes: violet – distal phalanx, red – middle (intermediate) phalanx, green – proximal phalanx, blue – metacarpal phalanx, black – carpals.

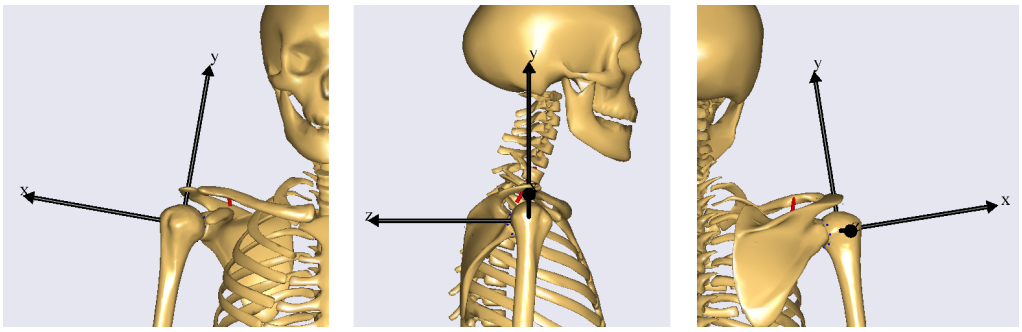

Figure 9: The local coordinate system of humerus. From the left: front view, right-side view, back view.

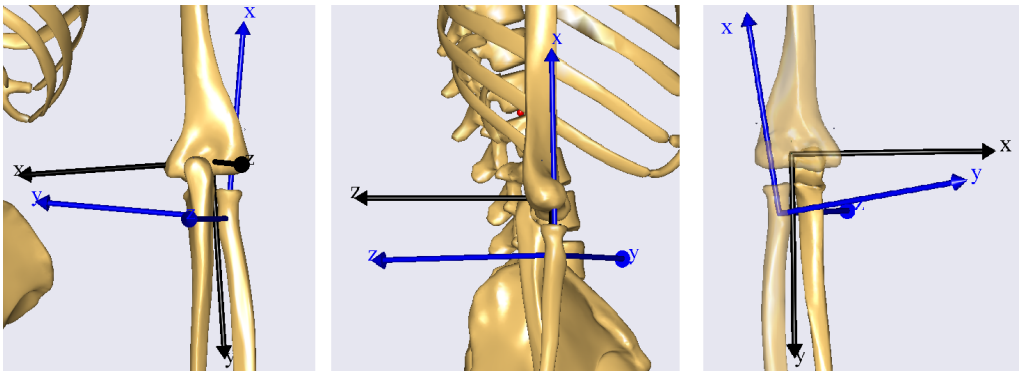

Figure 10: The local coordinate systems of ulna and radius. From the left: back view, right-side view, front view (transparent view of humerus and radius). Notes: black – ulna, blue – radius

4 Matlab code for calculating lines end and via points

Matlab code has single entry point `main.m` where you can specify input file, output folder and whether you want do display figures with plots of results. The input file is in `.yaml` format and contains:

- `Name`: name of the muscle to be used for output
- `K`: number of lines to use, can be a list
- `Surfs`: list of surfaces in desired order of connection saved as stl files, all with common coordinate system

Example of input file is included, see `abductor_digiti_minimi.yaml`.

References

[1] Hans-Hermann Bock. Origins and extensions of the k-means algorithm in cluster analysis. *Journal Electronique d'Histoire des Probabilités et de la Statistique*, 4(2):1–18, 2008.

[2] S. L. Delp, J. P. Loan, M. G. Hoy, F. E. Zajac, E. L. Topp, and J. M. Rosen. An interactive graphics-based model of the lower extremity to study orthopaedic surgical procedures. *IEEE Transactions on Biomedical Engineering*, 37(8):757–767, Aug 1990.

[3] András Frank. On Kuhn's Hungarian Method–A tribute from Hungary. *Naval Research Logistics (NRL)*, 52(1):2–5, 2005.

[4] J. MacQueen. Some methods for classification and analysis of multivariateobservations. In *Proceedings of the Fifth Berkeley Symposium on Mathe-matical Statistics and Probability, Volume 1: Statistics*, pages 281–297. University of California Press, Berkeley, Calif., 1967.

[5] Kevin B. Shelburne and Marcus G. Pandy. A musculoskeletal model of the knee for evaluating ligament forces during isometric contractions. *Journal of Biomechanics*, 30(2):163–176, 1997.

[6] H.E.J. Veeger, Bing Yu, Kai-Nan An, and R.H. Rozendal. Parameters for modeling the upper extremity. *Journal of Biomechanics*, 30(6):647–652, 1997.

[7] Jack M. Winters and Douglas G. Kleweno. Effect of initial upper-limb alignment on muscle contributions to isometric strength curves. *Journal of Biomechanics*, 26(2):143–153, 1993.

Acknowledgments

This work was supported by the project n. 182 "Obstetrics 2.0 – Virtual models for the prevention of injuries during childbirth" realised within the frame of the Program INTERREG V-A: Cross-border cooperation between the Czech Republic and the Federal State of Germany Bavaria, Aim European Cross-border cooperation 2014-2020. The realisation is supported by financial means of the European Regional Development Fund (85 % of the costs) and the state budget of the Czech Republic (5 %). KI is part-funded by project No. CZ.02.1.01/0.0/0.0/16_019/0000787 â€śFighting INfectious Diseasesâ€ś, awarded by the Ministry of Education, Youth and Sports of the Czech Republic, financed from The European Regional Development Fund.